

Voxel based calcification fraction quantification in atherosclerotic plaques using serial UTE

Jinnan Wang¹, Niranjana Balu², Thomas S Hatsukami², Chun Yuan², and Peter Börnert³

¹Philips Research North America, Briarcliff Manor, NY, United States, ²University of Washington, ³Philips Research Europe

Introduction Although MR has been shown to provide accurate and reliable atherosclerotic plaque components identification, the detection of high risk components is usually compromised when they coexist with calcification 1. Speckled calcification, which presents in over 35% of advanced plaques, usually coexists with high-risk plaque components at an arbitrary fraction. As a result, the MR signal from high risk components is masked by reduced signal from speckled calcification (Fig.1). The signal from the high-risk components can be corrected, in theory, if the fraction of calcification at a particular location is known. Currently, however, there is no technique available capable of accurate estimation of the calcification fraction on the voxel level. To address this gap, a serial UTE based magnetic resonance imaging and processing approach is proposed in this study to accurately quantify the calcification fraction on a voxel level.

Methods Six human endarterectomy specimens were scanned using a clinical 3T scanner (Philips Achieva, R2.61, the Netherlands) with a solenoid coil for improved SNR. Seven 3D radial UTE images with different TEs (TE = 0.1, 0.2, 0.4... 6.4ms) were acquired to measure the calcification fraction at each location. Other imaging parameters were: T1-FFE, TR 25ms, FA 12°, FOV 28×28×28mm³, resolution: 0.25×0.25×0.25mm³, 40% radial sampling rate, fat saturation, imaging time of each acquisition: 4min26sec.

The signal intensity value at each voxel is given by a bi-exponential decay model:

$$S_i = \lambda_1 \exp(-TE_i / T_{2\text{short}}) + \lambda_2 \exp(-TE_i / T_{2\text{regular}}) \quad i=1,2,\dots,7 \quad (\text{Eq.1})$$

Where $\lambda_{1,2}$ are the relative signal weightings of the short and regular T_2 components and T_{2s} are the values of short and regular T_2 components. Knowing the proton density difference between calcification and soft tissue is $\sim 1:5^{2,3}$, calcification fraction at each voxel can be determined based on the ratio between different λ s.

Due to the signal variation at each voxel, Eq.1 cannot always be reliably estimated by a least square approach. A non-linear mixed effect (NLME) model (4) was adopted to account for non-constant correlation among different voxels, making the model more robust to the presence of noise. In the NLME model, each observation is represented as a combination of a fixed response, an individual response and a random error:

$$\begin{cases} S_{i,j} = f(\kappa_j) + \varepsilon_j, & \varepsilon_j \sim N(0, \sigma^2) \\ \kappa_j = g(\beta, b_j), & b_j \sim N(0, \sigma^2) \end{cases} \quad (\text{Eq.2})$$

where j represents different voxels, $f(\kappa_j)$ is the original function, $g(\beta, b_j)$ is the parameter estimation function, ε is the residual error, κ_j is the vector including all parameters in Eq.1, β is the fixed effect parameter, b_j is the inter-voxel variability. As the mean value is determined on a population basis, no initial value needs to be provided for NLME modeling.

The slice with the maximum calcification area from each specimen was analyzed using the NLME model. Only pixels contained calcification were included in the analysis using interactive region of interest (ROI) selection. The calcification fraction of all voxels was plotted in a histogram to examine the calcification distribution. Pearson's correlation between MR signal intensity at TE=0.1ms and measured calcification fraction was calculated to examine the agreement between the two.

Results Successful NLME fitting was obtained for over 95% of all included voxels, compared to $\sim 50\%$ when the least square approach is used. An example comparison of fitting results is shown in Fig.2: the NLME model demonstrated more successful fitting on the same dataset. Color-coded calcification map overlaid on the original MR images showed robust calcification fraction measurement without noticeable fitting noise (Fig. 3b). Furthermore, the signal variation pattern on calcification maps corresponds to well to that on the original MR images.

When plotted against the original signal intensity on MR images, a good correlation ($r=-0.73$, $p<0.01$) was obtained (Fig.4). When the calcification fraction is high (over 70%), there was a good correlation between high calcification and low signal intensity, indicating that the signal was dominated by calcification. When the calcification fraction was low, however, the distribution became more spread out, indicating the signal was more dominated by the other tissues coexisting in the same voxel.

In conclusion, the feasibility of measuring calcification fraction on a voxel level has been demonstrated in this study. Robust calcification fraction maps can be generated using the NLME model. This approach can also be applied to other applications where the accurate quantification of calcification on a pixel/voxel level is needed.

References: 1. Ota et al. Radiology 2010. 2. Du et al. MRM 2011. 3. Rajanayagam et al. MRI 1991. 4. Lindstrom and Bates, Biometrics, 1990.

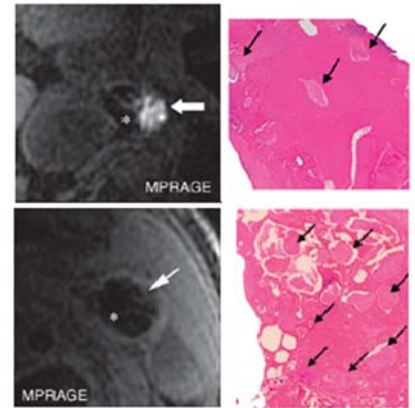


Fig. 1 Disparate MR signals of IPH on plaques with different calcification content identified by histology. Upper row: IPH is bright when calcification content is low; Lower row: IPH is dark when calcification content is high.

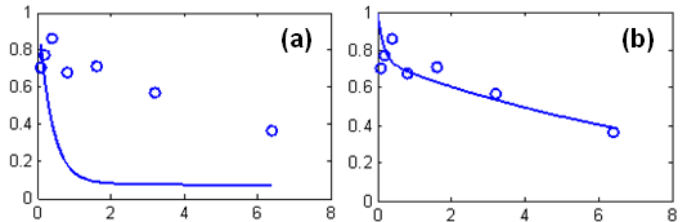


Fig. 2 Sample fitting results from regular least-square approach (a) and the NLME model (b) on the same dataset. A more successful fitting can be observed when the NLME model was applied.

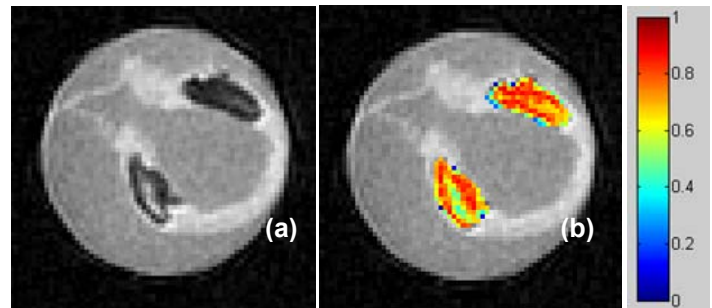


Fig. 3 MR image (a) and the corresponding calcification map (b) obtained from serial UTE images; the colorbar shows the calcification fraction. Note the level of continuity on the colored calcification maps.

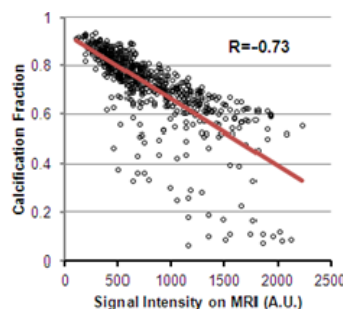


Fig. 4 Scatter plot between the signal intensity on MR images and the calcification fraction measured by the NLME model. A good correlation ($R=-0.73$, $p<0.001$) was found between the two.